ELSEVIER

Marine Geology 193 (2003) 151–169

MARINE GEOLOGY
INTERNATIONAL JOURNAL OF MARINE GEOLOGY, GEOCHEMISTRY AND GEOPHYSICS

www.elsevier.com/locate/margeo

# Modelling long-term tidal marsh growth under changing tidal conditions and suspended sediment concentrations, Scheldt estuary, Belgium

S. Temmerman [a,*], G. Govers [a], P. Meire [b], S. Wartel [c]

[a] *Laboratory for Experimental Geomorphology, Katholieke Universiteit Leuven, Redingenstraat 16, 3000 Leuven, Belgium*
[b] *Ecosystem Management research group, University of Antwerp, Universiteitsplein 1-c, 2610 Antwerp, Belgium*
[c] *Sedimentology Department, Royal Belgian Institute of Natural Sciences, Vautierstraat 29, 1000 Brussels, Belgium*

Received 21 November 2001; received in revised form 6 November 2002; accepted 7 November 2002

**Abstract**

Existing numerical models simulating the vertical growth of tidal marshes have only, to a very limited degree, been validated using observed data. In this study, we describe a refined zero-dimensional time-stepping model, which is based on the mass balance approach of Krone [in: Coastal Sediments '87, 1987, pp. 316–323], Allen [Mar. Geol. 95 (1990) 77–96] and French [Earth Surf. Process. Landforms 18 (1993) 63–81]. The model is applied and evaluated, using field data on suspended sediment and tidal regime as input and the historical growth of a specific minerogenic tidal marsh in the Scheldt estuary (Belgium) as independent data for model testing. First, the historical rise of the marsh surface during the past 55 years is reconstructed based on land use and vegetation cover changes, which are dated using aerial photographs and which are recognised in sediment cores. After marsh formation, the marsh surface builds up very quickly and asymptotically to an equilibrium level relative to the tidal frame. Second, temporal variations in suspended sediment concentration (SSC) were measured above the actual marsh surface during a 1-year period. These measurements show that the SSC, in the water that floods the marsh surface at the beginning of an inundation, increases linearly with maximum inundation height. The application of existing models, which assume a constant incoming SSC, leads to an underestimation of the observed historical growth and to biased predictions under scenarios of future sea-level rise. However, after incorporation of the relationship between SSC and inundation height, the observed vertical growth is successfully simulated. This leads to the conclusion that not only the decrease in tidal inundation, but also the decrease in SSC with decreasing marsh inundation height, is of great importance to fully explain and successfully simulate the long-term vertical morphodynamics of tidal marshes.


*Keywords:* tidal marshes; numerical modelling; sediment deposition; morphodynamics; Scheldt estuary

## 1. Introduction

Tidal marshes are widely recognised as net sinks of sediment, which leads, in the long term, to vertical rise or growth of tidal marsh platforms

* Corresponding author. Tel.: +32-16-326407; Fax: +32-16-326400.
*E-mail address:* stijn.temmerman@geo.kuleuven.ac.be (S. Temmerman).

0025-3227/02/$ – see front matter 
PII: S0025-3227(02)00642-4

and which is the major factor that controls changes in the ecological and economic functions of tidal marshes (Allen and Pye, 1992; Reed, 1993). Numerous field studies have been conducted on sediment accretion in tidal marshes on time-scales of less then 100 years, using a wide range of measuring techniques (see Allen (1990), French and Spencer (1993) and Allen (2000) for an overview). An important insight in the growth pattern of tidal marshes on time-scales of the order of $10^2$–$10^3$ years comes from the study of Pethick (1981). He observed an asymptotic relationship between marsh surface elevation and age for the salt marshes of north Norfolk (UK), from which he concluded that young tidal marshes are rapidly built up. As the marsh surface rises higher within the tidal frame and is consequently less flooded, the growth rate decreases and the marsh surface finally tends to an equilibrium level high in the tidal frame (Pethick, 1981). This negative feedback mechanism between elevation and growth rate is widely assumed to be the most important mechanism controlling the long-term vertical growth of tidal marshes (e.g. Letzsch and Frey, 1980; Allen, 1990; 2000; French, 1993). When the marsh surface is in equilibrium with the tidal frame and continues to aggrade under rising sea level, the growth rate is assumed to be equal to the rate of sea-level rise (e.g. Allen, 1990; Shi, 1993; Orson et al., 1998). In many places, however, it was found that tidal marshes are not able to keep up with rising sea level (Reed, 1995; Ward et al., 1998), resulting in submergence and major losses of tidal marsh areas (Baumann et al., 1984; Walker et al., 1987; Kearny and Stevenson, 1991).

A relatively small number of physically based numerical models were developed to simulate and to help understand long-term (50–$10^3$ years) vertical marsh dynamics. These models are based on a zero-dimensional time-stepping modelling approach, to simulate the vertical growth of marsh platforms with time at one point that is considered representative for the whole platform (Krone, 1987; Allen, 1990; 1995; 1997; French, 1993). On shorter time-scales (1 year) spatial variations in sedimentation rate within a marsh are significant (French and Spencer, 1993; French et al., 1995; Leonard, 1997) and a one- or two-dimensional spatially distributed modelling approach has to be used (Allen, 1994; Woolnough et al., 1995). For longer time-scales (50–$10^3$ years), however, the general flat topography of marsh platforms suggests that the zero-dimensional approach is acceptable. The existing models of Krone (1987), Allen (1990), and French (1993) are all based on the same basic principle of a negative feedback between marsh surface elevation and frequency of tidal inundation. A simple mass-balance approach is used, since the complex flow structure in and over the marsh vegetation and complex variations in suspended sediment supply and settling velocity are still poorly understood (e.g. Pethick et al., 1990; Leonard and Luther, 1995; Shi et al., 2000). Krone (1987) proposed a zero-dimensional mass-balance model, which was used to simulate the response of tidal marshes in San Francisco Bay to historical sea-level change. These simulations showed that marsh surfaces only attain a relative equilibrium level after the rate of sea-level rise becomes constant. French (1993) followed a similar modelling approach to simulate marsh response to regional subsidence and to several scenarios of future sea-level rise along the barrier-coast of north Norfolk (UK). Allen (1990) conducted a series of numerical experiments on the long-term vertical growth of Holocene salt marshes in the Severn estuary (UK), under different rates of sea-level change and of organic sediment deposition. With a similar modelling scheme Allen (1995, 1997) also simulated the succession of minerogenic to organogenic marshes and the expansion and shrinkage of marsh creek networks, when sea level fluctuates about an underlying upward trend.

However, as indicated by Allen (1997), the model applications described above are rather exploratory and were especially conducted to investigate the general long-term behaviour of tidal marshes. They were only validated to a very limited degree using observed data, so that the results are only qualitatively valid. This paper aims to evaluate a refined zero-dimensional time-stepping model for vertical marsh growth. First, the historical growth at two locations within a specific minerogenic tidal marsh is reconstructed using field

data and is used as an independent data set for model testing. Second, the input parameters for the model are obtained by extensive short-term field measurements of the suspended sediment regime at the actual marsh surface. The implementation and evaluation of the model shows that an important modification of the existing models is necessary to obtain model predictions that are in good agreement with long-term field observations.

## 2. The study area

The Scheldt estuary is situated in the southwest of the Netherlands and the northwest of Belgium and reaches over 160 km from the mouth in the southern North Sea up to Ghent (Fig. 1; see Meire et al. (1992), Baeyens et al. (1998) and Van Damme et al. (2001) for a more detailed description of the Scheldt estuary). The Dutch and Belgian parts of the estuary are called the Western Scheldt and the Sea Scheldt, respectively. The hydraulic regime of the estuary is characterised by a semidiurnal meso- to macrotidal regime. During spring and neap tides, the mean tidal range at the mouth is 4.46 and 2.97 m, respectively. As the tides enter the estuary, these mean tidal ranges increase to 5.93 and 4.49 m near Rupelmonde and then decrease farther inland to 2.24 and 1.84 m in Ghent. The most extreme high-water levels are caused by storm surges coming from the North Sea during periods of strong northwesterly winds and can be 2–3 m higher than mean high-water levels (Claessens and Meyvis, 1994).

The suspended sediment in the Scheldt estuary mainly consists of fine sand and mud, with concentrations typically showing large spatial and temporal variations. The time-averaged longitudinal concentration profile is characterised by low concentrations in the Western Scheldt (30–60 mg/l) and a turbidity maximum situated between the Dutch–Belgian border and Temse, with mean concentrations of 100–200 mg/l (e.g. Van Damme

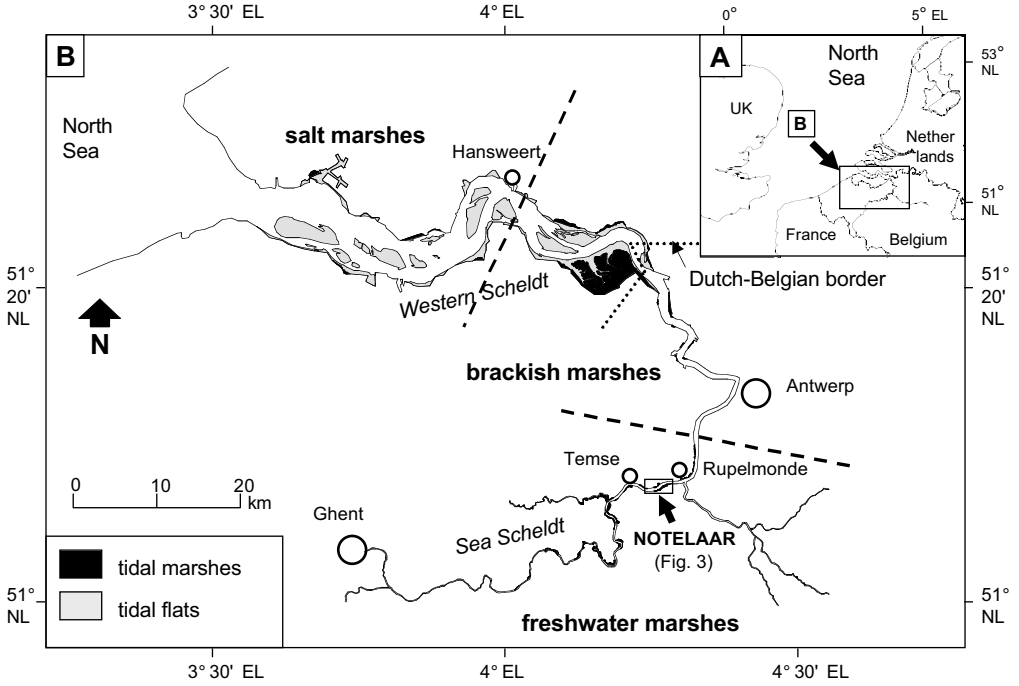


Fig. 1. The Scheldt estuary. (A) Location within Western Europe. (B) Location of salt, brackish and freshwater tidal marshes (areas separated by heavy dashed lines) together with the study area, the Notelaar marsh, and places named in the text. A more detailed map of the Notelaar marsh is shown in Fig. 3d.

et al., 2001; Van Eck et al., 1991). Farther upstream the suspended sediment concentrations again slightly decrease to 50–100 mg/l (Van Damme et al., 2001). There are also large temporal variations in sediment concentration and in the position of the turbidity maximum, depending on the tides and the freshwater discharge, which vary over semidiurnal, spring–neap and seasonal time-scales (Fettweis et al., 1998).

The tidal marshes of the Scheldt estuary can be classified into salt, brackish and freshwater tidal marshes, according to the salinity gradient, which exists along the estuary (Fig. 1b). The study area, the Notelaar marsh, is located in the most seaward part of the freshwater zone, nearly 4 km downstream from Temse. The Notelaar marsh has a total area of 27 ha and covers a length of 2 km along the stream channel of the Scheldt estuary. It typically consists of a vegetated marsh platform, with elevation differences never greater than 0.30–0.40 m, and is dissected by tidal creeks that branch, narrow and shallow inland. The marsh is situated in the zone where the tidal range and suspended sediment concentrations attain their largest values along the Scheldt estuary. Local tidal water levels are represented in Fig. 2, in relation to the marsh surface elevation. The vegetated marsh platform is only flooded during spring tides, while the unvegetated tidal mud flat, which borders the marsh, is flooded during every high tide. The Notelaar marsh vegetation consists of typical freshwater tidal marsh plants, consisting of *Phragmites australis* in the lower elevations of the marsh and a community of *Salix* sp. in the higher elevations (Fig. 3d). Both plant communities are abundant, producing a very dense vegetation cover. In these freshwater tidal marshes, *Phragmites australis* reaches exceptional heights of up to 4 m.

## 3. Materials and methods

### 3.1. Assessment of historical long-term morphodynamics

The morphodynamics at the Notelaar marsh during the past five decades was reconstructed using a combination of two methods: (1) the interpretation of aerial photographs of different ages, and (2) sampling and analysis of undisturbed sediment cores.

The Notelaar marsh is covered by 10 aerial photograph series, which date from 1944 to 1998. These photos of successive age clearly illustrate how the geomorphology, land use, and vegetation cover changed during the past five decades. Four maps were made, based on four aerial photograph series (1944, scale 1:16 800; 1951, 1:18 000; 1965, 1:10 000; and 1998, 1:10 000) that illustrate all changes in land use or vegetation cover that occurred at the Notelaar marsh over this time period (Fig. 3).

Based on vegetative changes observed from aer-

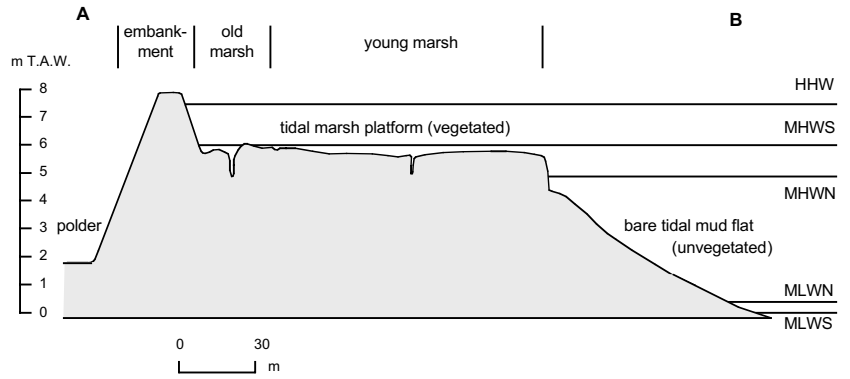


Fig. 2. Topographic profile across the Notelaar marsh (see Fig. 3d for location of profile A–B). Local tidal water levels are indicated relative to Belgian Ordnance Level (T.A.W.) (HHW = highest high-water level; MHWS and MHWN = mean high-water level at spring and neap tides, respectively; MLWN and MLWS = mean low-water level at neap and spring tides, respectively).

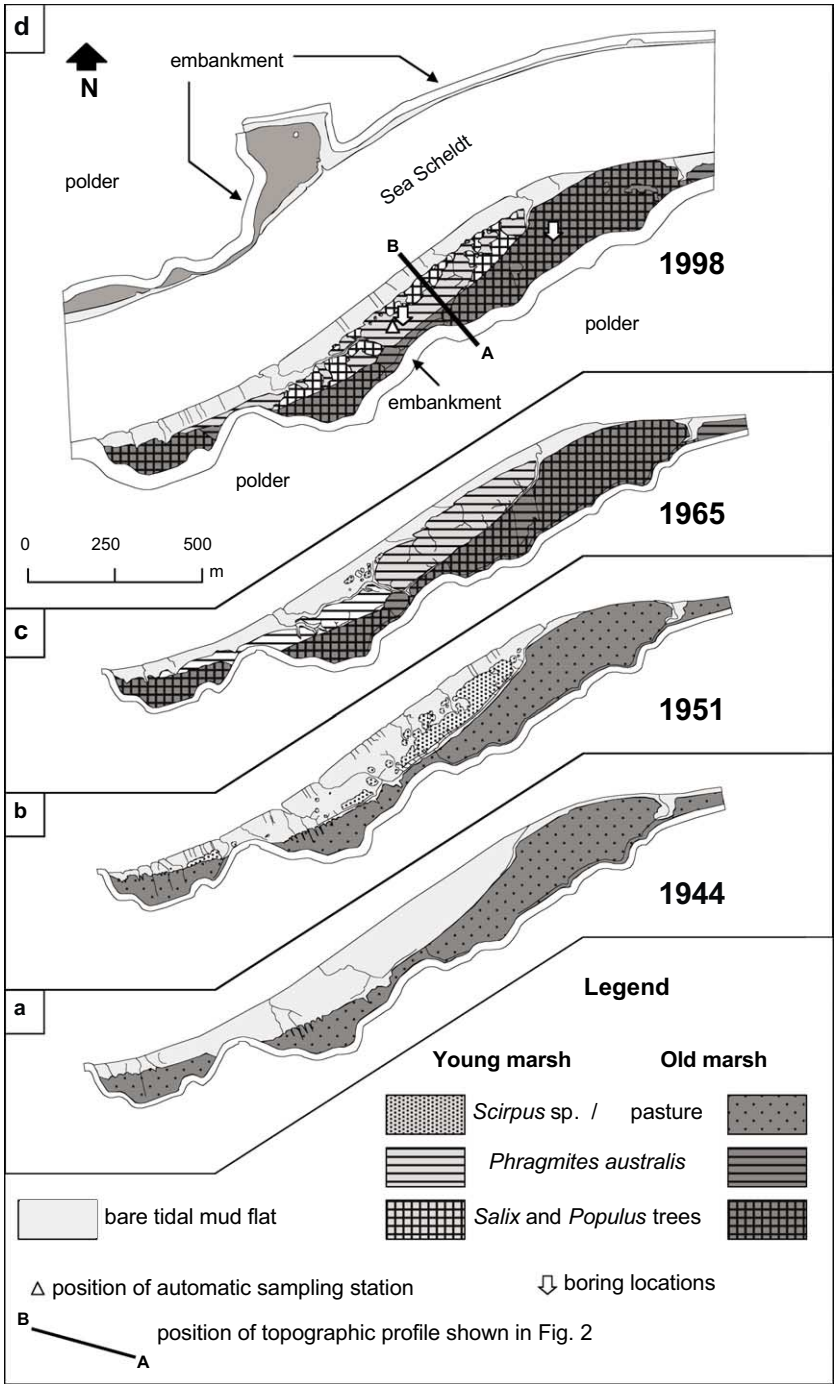


Fig. 3. Reconstruction of the land use and vegetation cover types that succeeded in time at the Notelaar marsh, based on aerial photographs dating back to (a) 1944, (b) 1951, (c) 1965 and (d) 1998; on this last map the position of the automatic sampling station, the cross-section in Fig. 2 and the boring locations at the young and old marsh are also indicated.

ial photographs, two marsh sections can be distinguished, which are further referred to as the young and old marsh. From both marsh sections undisturbed sediment cores were collected with a 'Beeker-sampler', a piston corer with thin-walled tubes of 5.7 cm in diameter and 150 cm in length and an inflatable valve at the bottom that prevents sediment loss while raising the corer to the surface. Both at the young and old marsh, a series of five replicate cores was collected within a small boring area of no more than 8 by 8 m (Fig. 3d). The marsh surface elevation at both boring locations was measured, relative to the fixed datum of the Belgian levelling network (T.A.W. or Tweede Algemene Waterpassing). All sediment cores were analysed in 1 cm sections to identify the plant debris that was preserved within the deposited sediment. Only plant debris of above-ground origin was considered (i.e. no roots, but only leaves and stems), and this debris was assumed to be deposited in situ. The floating-in of debris originating from distant marsh sections with a different vegetation cover is very unlikely, because the dense and 2–4 m high vegetation cover prevents large displacement of plant detritus during tidal inundations, which are only exceptionally higher than 1.5 m. In this way, we identified for each boring location sediment layers containing different plant debris, which could be related to the different land use or vegetation cover types that succeeded each other in time at the specific boring location.

The contact elevation between sediment layers with different plant debris corresponds in time to the historic marsh surface elevation at the moment of land use/vegetation cover change. This change was then dated using the aerial photographs. In this way, a series of time–elevation points was determined. The error on the contact elevations was estimated by the standard deviation, as determined from the five replicate cores, and was found to be low (between 3.3 and 6.4

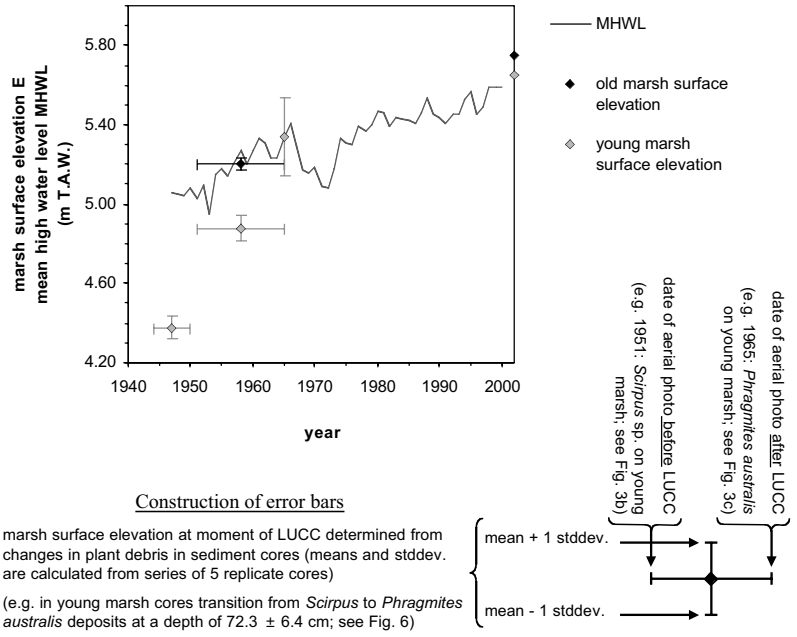


Fig. 4. Observed vertical growth of the old and young marsh of the Notelaar. Construction of time-elevation points is based on land use or vegetation cover changes (LUCC), which could be dated using aerial photos (see Fig. 3) and the marsh surface elevation at that moment was derived from sediment cores (see Fig. 6). The construction of error bars is explained in the lower part of this figure (error bars for the 2002 data points, which are the measured present-day marsh elevations, are $<0.01$ m and are therefore not shown). MHWL = yearly mean high-water level (Waterways and Maritime Affairs Administration of the Flemish Community).

cm). The error on the dating of the historic land use/vegetation cover change, with which a contact elevation is associated, is determined by the time interval between successive aerial photos before and after the land use or vegetation cover change (see also Fig. 4). Finally, from these time–elevation points a long-term historical growth rate of the marsh surface was calculated.

For comparison, recent accumulation rates were measured at four locations (two close to each of both boring locations) using white feldspar marker horizons of 60 by 60 cm, placed on the marsh surface on 30/03/2000. Thickness of sediment deposits was estimated after 2 years by the mean and standard deviation of six measurements above each marker horizon, using a small gauge (diameter = 1.5 cm).

### 3.2. Measurement of actual sediment dynamics

During a 1-year period (April 2000–April 2001), temporal variations of suspended sediment concentration in the flooding water were measured, using an automatic sampling station, located at the boring location on the young marsh (see Fig. 3d). For every tidal inundation during the year, the water level above the marsh surface was measured automatically every 5 min with an ISCO flowmeter 4220 and saved as digital time–inundation height data. At the same time, samples from the flooding water were automatically pumped up from a sampling point, located at 0.15 m above the marsh surface, and stored in 1 litre bottles with an ISCO sampler 6700. The sampler and flowmeter were programmed in such a way that, once the inundation height was higher than 0.15 m, a first sample was taken. Subsequent samples were collected every 30 min, until the water level was again below 0.15 m above the marsh surface. This sampling routine was repeated for each inundation cycle during the 1-year measuring period. Every 15 days (after each neap–spring–neap tidal cycle) the filled bottles were collected and replaced by empty ones. In the laboratory, water samples were filtered with filter papers (pore diameter = 0.45 μm) to determine the suspended sediment concentration (SSC in g/l). In order to reduce the laboratory work, samples of only four or five tidal inundation events were analysed for each spring–neap cycle so that the full range of low to maximum inundation events during that spring–neap cycle was covered. In all, 194 samples were analysed, covering 102 tidal inundations spread over 25 spring–neap cycles or 27% of the total number of inundation events during the 1-year measuring period.

### 3.3. Description of the numerical model

Following the zero-dimensional time-stepping models of Allen (1990, 1995, 1997) and French (1993), the rate of change in marsh surface elevation $E$ (in m relative to a fixed datum) at a certain point may be written as:

$$\mathrm{d}E/\mathrm{d}t = \mathrm{d}S_{\mathrm{min}}/\mathrm{d}t + \mathrm{d}S_{\mathrm{org}}/\mathrm{d}t - \mathrm{d}P/\mathrm{d}t \quad (1)$$

where $\mathrm{d}S_{\mathrm{min}}/\mathrm{d}t$ is the rate of mineral sediment deposition, $\mathrm{d}S_{\mathrm{org}}/\mathrm{d}t$ the rate of organic sediment deposition and $\mathrm{d}P/\mathrm{d}t$ is the rate of compaction of the deposited sediment, after dewatering, under younger sediment load. All terms are in m/yr.

The yearly rate of mineral sediment deposition $\mathrm{d}S_{\mathrm{min}}/\mathrm{d}t$ is further specified as (after Krone, 1987):

$$\frac{\mathrm{d}S_{\mathrm{min}}}{\mathrm{d}t} = \int_{\mathrm{year}} \int_{T} \frac{w_{\mathrm{s}} C(t)\,\mathrm{d}t}{\rho} \quad (2)$$

Sediment deposition is here classically modelled as the product of a characteristic settling velocity $w_{\mathrm{s}}$ (in m/s) and the depth-averaged concentration $C$ (in g/l or kg/m$^3$) of the suspended sediment above the marsh surface. During one tidal inundation, $C$ varies with time $t$. In order to obtain the thickness of the deposited sediment layer, this product is divided by the dry bulk density $\rho$ (in kg/m$^3$) of the inorganic surface sediment, after dewatering over spring–neap and seasonal timescales. This deposition term is first integrated over the total duration $T$ of one tidal inundation and then over all inundations during a year. Eq. 2 ignores the existence of a vertical sediment concentration gradient in the water column overlying the marsh surface, and assumes that there is no resuspension of sediment, once it has settled to

the marsh surface. These assumptions are acceptable, because the inundation heights and flow velocities above the marsh surface are typically low, due to the very flat topography and hydraulic resistance by the dense and high marsh vegetation.

The temporal variation $C(t)$ during one inundation is modelled using the following mass balance equation:

$$\frac{\mathrm{d}[h(t)-E]C(t)}{\mathrm{d}t} = -w_s C(t) + C(0)\frac{\mathrm{d}h}{\mathrm{d}t} \quad (3)$$

where $h(t)$ is the time-dependent water surface elevation, $E$ is the elevation of the marsh surface for a given year and $C(0)$ is the sediment concentration (in kg/m$^3$) in the flooding water. $h(t)$ and $E$ are expressed in m relative to a fixed datum. Eq. 3 describes the change in suspended sediment mass above a unit area of the marsh surface (first term), as a result of the vertical settling of suspended sediment (second term) and lateral flux of water with a suspended sediment concentration $C(0)$ (third term). $C(0)$ will have a specific value during the flood tide (when $\mathrm{d}h/\mathrm{d}t > 0$), while during the ebb tide (when $\mathrm{d}h/\mathrm{d}t < 0$) $C(0)$ is set to equal $C(t)$. This equation also assumes that there is no resuspension after sediment deposition. Further derivation of Eq. 3 leads to the mass balance equation that was proposed by Krone (1987) and also used by French (1993):

$$[h(t)-E]\frac{\mathrm{d}C}{\mathrm{d}t} = -w_s C(t) + [C(0)-C(t)]\frac{\mathrm{d}h}{\mathrm{d}t} \quad (4)$$

The function $h(t)$, describing the temporal variation of the water level within one semidiurnal tidal cycle, is modelled using the average tidal curve at Temse (Fig. 5a), where the nearest tide-gauge station of the Waterways and Maritime Affairs Administration is located (nearly 4 km upstream from the Notelaar marsh). We suppose that this mean tidal curve simply moves up or down as the high-water level is higher or lower. This simplification is acceptable because only the uppermost portion of the tidal curve floods the marsh surface. $h(t)$ can then be calculated for any tidal inundation with a high-water level $h(t_{HW})$ as:

$$h(t) = a\frac{1}{1+\left(\frac{t-x_0}{b}\right)^2} + h(t_{HW}) - h(t_{MHW}) \quad (5)$$

where $a$, $b$ and $x_0$ are constants ($a = 5.3787$; $b = 10837.0147$; $x_0 = 220.2821$) and $h(t_{MHW})$ = the mean high-water level (= 5.44 m T.A.W. at Temse; Claessens and Meyvis, 1994).

From Eqs. 5, 3 and 2, $\mathrm{d}S_{min}/\mathrm{d}t$ can now be computed for single tidal inundations with a certain high-water level $h(t_{HW})$. To calculate the total sedimentation rate $\mathrm{d}S_{min}/\mathrm{d}t$ for every year in the simulation period, the frequency distribution of high-water levels has to be simulated for every year. To do this we used the observed evolution of yearly mean high-water level (MHWL) at Temse and the yearly-averaged frequency distribution of high-water levels around MHWL at Antwerp, which is the nearest tide-gauge station

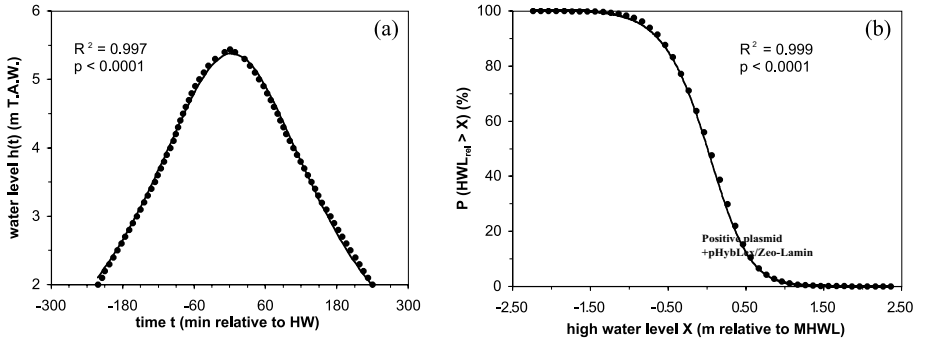


Fig. 5. (a) Observed (dots) and modelled (line) mean tidal curve at Temse for the period 1981–1990. (b) Observed (dots) and modelled (line) high-water frequency distribution at Antwerp for the period 1981–1990 (all observed data are supplied by the Waterways and Maritime Affairs Administration of the Flemish Community).

where these data are available (Claessens and Meyvis, 1994). This frequency distribution is modelled as (Fig. 5b):

$$P(\mathrm{HWL_{rel}}>X) = y_0 + \frac{a}{(1+\mathrm{e}^{-(X-x_0)/b})^c} \quad (6)$$

where $\mathrm{HWL_{rel}}$ is the high-water level relative to mean high-water level (in m) and $a$, $b$, $c$, $x_0$ and $y_0$ are constants (here $a=100.5877$, $b=-0.3160$, $c=1.7014$, $x_0=0.2414$ and $y_0=-0.0017$). $P$ is expressed in percent.

The above-described simulation model was programmed as a routine in Matlab, solving Eqs. 5, 3 and 2 in time-steps of 300 s and Eq. 1 in time-steps of 1 year. In this modelling study, the observed long-term vertical growth of the Notelaar marsh was simulated in order to test the model. The assessment of representative values for the model input parameters was based on the results of the short-term field measurements.

## 4. Results

### 4.1. Observed long-term morphodynamics

The aerial photographs of the Notelaar marsh show that the present-day marsh consists of two sections: an old marsh, which is already present on the photographs of 1944, and a young marsh, which started to form between 1944 and 1951 (Fig. 3). As the old marsh is already shown on the topographic maps of De Ferraris (1774–1777) and Vandermaelen (1846–1854), it must have formed before the end of the 18th century. These maps indicate that the old marsh was then used as a pasture. The aerial photographs of 1944 and 1951 show that the old marsh surface was then divided into lots and covered by low grassy vegetation, which leads to the conclusion that the old marsh was still used as a pasture (Fig. 3a,b). By 1965, the pasture had disappeared and was replaced by trees, mainly *Salix* and possibly also *Populus* sp. (Fig. 3c). The rectilinear growing pattern of these trees indicates that they were planted for the cultivation of willow withes, which was very common along the Sea Scheldt until the end of the 1960s (Durinck, 1981). Since then an abandoned *Salix* and *Populus* vegetation cover developed at the old marsh (Fig. 3d).

In contrast, the young marsh has a different history. Comparison of aerial photos shows that the young marsh was not yet formed in 1944, and instead, an unvegetated tidal flat existed (Fig. 3a,d). By 1951, a large part of this tidal flat was colonised by *Scirpus* sp., typically growing in concentric patterns (Fig. 3b), which forms the initial stage of the natural vegetation succession of freshwater tidal marshes within the Scheldt estuary (Hoffmann, 1993). By 1965, almost all of the *Scirpus* plants were replaced by a dense, closed *Phragmites australis* cover, the next phase of the natural vegetation succession (Fig. 3c). Between 1965 and 1998, some *Salix* trees expanded from the old marsh to the young marsh, especially on the natural levees which developed along the streamside border of the young marsh and along the main tidal creeks. However, at present, *Phragmites australis* remains the dominant plant species over a large portion of the young marsh (Fig. 3d).

Both at the young and old marsh, five undisturbed sediment cores were collected, and the macroscopic plant debris in the cores was identified (Fig. 6). For the old marsh, the upper sediment layer (to a depth of $49.8\pm3.3$ cm) contains woody plant debris and oblong leaves as a consequence of accumulation under the *Salix* vegetation. Deposits below this level contain no woody plant debris but only small remains of grasses (Fig. 6), indicating that these sediments were deposited while the old marsh was still under pasture. For the young marsh, the recent *Phragmites australis* phase is characterised by remains of cylindrical hollow stems (Fig. 6). Below $72.3\pm6.4$ cm, the macroscopic plant debris is totally different and consists of large amounts of dark-coloured tubers and remains of three-cornered stems, typical for *Scirpus maritimus*. This sharp boundary between *Phragmites australis* and *Scirpus* deposits is also observed at the same elevation in the cliffs that border the young marsh platform. Finally, below $122.4\pm5.8$ cm depth no plant remains are found anymore, indicating that this sediment was deposited when the young marsh was not yet formed, and instead, an unvegetated tidal flat existed.

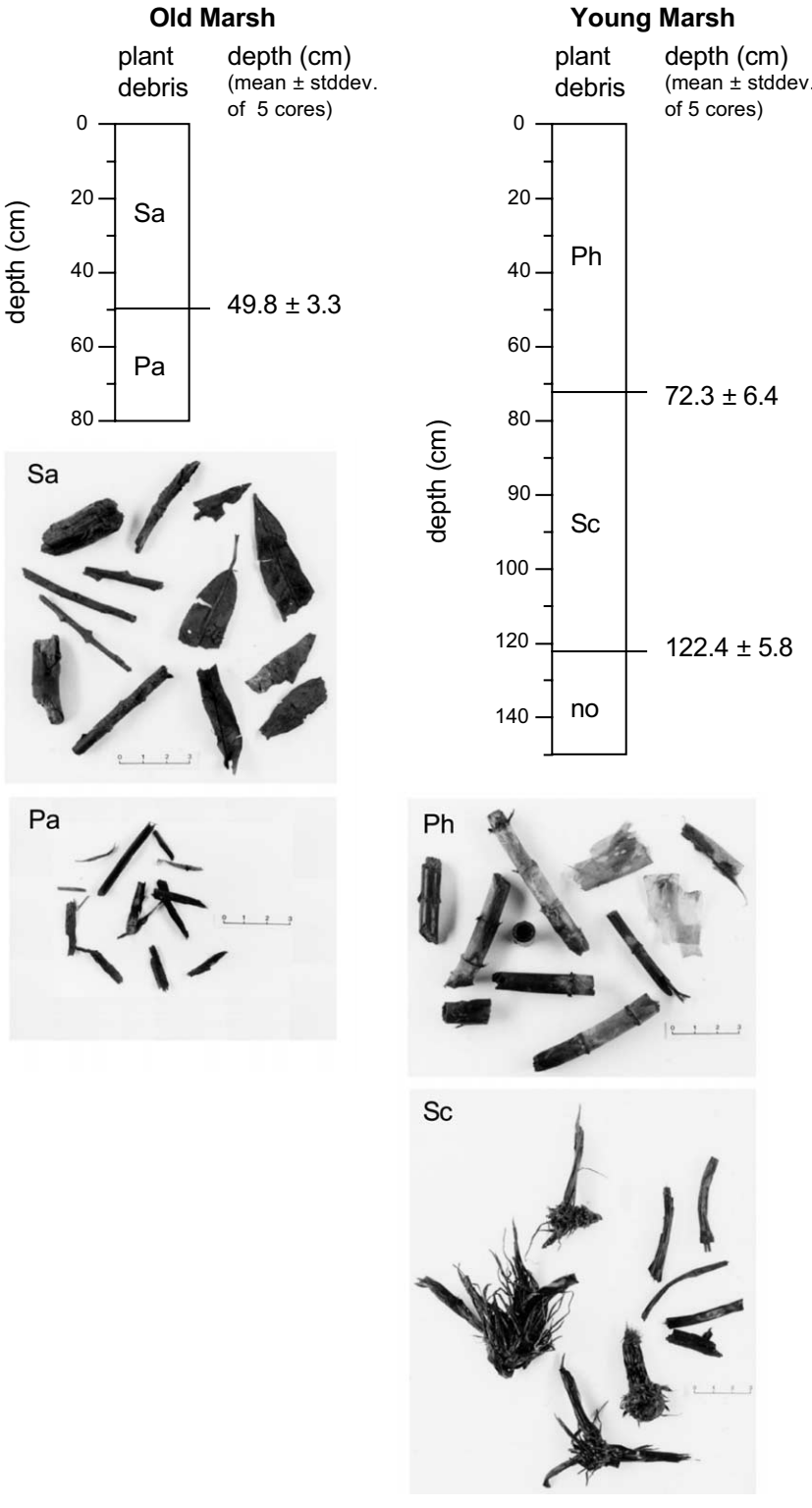
Old Marsh
plant debris
depth (cm) (mean ± stddev. of 5 cores)
depth (cm)
0
20
40
60
80
Sa
Pa
49.8 ± 3.3
Sa
Pa
Young Marsh
plant debris
depth (cm) (mean ± stddev. of 5 cores)
depth (cm)
0
20
40
60
80
90
100
120
140
Ph
Sc
no
72.3 ± 6.4
122.4 ± 5.8
Ph
Sc

Each contact level between these sediment layers was dated using the aerial photographs, resulting in a set of time–elevation points for the young and old marsh (Fig. 4). One additional point was added to Fig. 4: extensive vegetation surveys on the freshwater marshes of the Sea Scheldt showed that *Phragmites australis* occurs at MHWL ± 0.2 m (mean ± standard deviation of 50 observations; Criel et al., 1999). On the young marsh of the Notelaar, *Phragmites australis* was first observed on the aerial photographs of 1965. This allows us to construct an additional time–elevation point on Fig. 4.

Fig. 4 shows that the young marsh started to grow between 1944 and 1951 at an elevation clearly below that of the old marsh. The first colonisation of the bare tidal mud flat by *Scirpus* sp. was situated at a level of 68.4 ± 5.8 cm below mean high-water level at that time (MHWL in black line in Fig. 4). This is in agreement with the present-day observed appearance of *Scirpus* along the freshwater zone of the Scheldt estuary at a level of 0.6–1.7 m below MHWL (Hoffmann et al., 1997). After this *Scirpus* colonisation, the young marsh quickly accumulated to a level only about 0.3 m below MHWL, at a mean accumulation rate of 4.6 ± 3.2 cm/yr between 1947 and 1958. During the period 1958–2002, the young marsh aggraded slower (1.8 ± 0.3 cm/yr), at a rate only slightly higher than that of the old marsh (1.2 ± 0.2 cm/yr), which is in equilibrium with MHWL rise (on average 1.0 cm/yr; Fig. 4). The actual accumulation rates, as measured with feldspar marker horizons, are 1.6 ± 0.1 and 1.6 ± 0.2 cm/yr for the young marsh and 1.5 ± 0.4 and 1.3 ± 0.2 cm/yr for the old marsh. Although these accumulation rates were measured over only 2 years, they are in good agreement with the above-mentioned long-term accumulation rates.

### 4.2. Short-term temporal variations in suspended sediment concentration

Field measurements of the temporal variation in suspended sediment concentration (SSC) above the marsh surface show that the SSC generally decreases with time during a tidal inundation cycle (Fig. 7), which is a consequence of settling of the suspended sediment. The initial SSC (i.e. the SSC at the beginning of an inundation cycle at the moment that the inundation height exceeds 0.15 m) varies, however, from one tide to another. Fig. 8 shows this variation of the initial SSC (ISSC) as a function of the maximum inundation height at high water for every inundation cycle that was sampled. A positive linear relationship is observed between ISSC and maximum inundation height: as the marsh is submerged by higher tides, the flooding water apparently has a higher capacity to transport suspended sediment, so that the ISSC is higher.

In addition, this increase of ISSC with maximum inundation height is much greater during the winter (Oct.–Mar.) than during the summer period (Apr.–Sept.). This observation appears to be consistent with observed seasonal variations in SSC in the stream channel of the Scheldt estuary, which are generally attributed to seasonal variations in freshwater discharge, biological activity, wind regime, and terrestrial erosion (e.g. Fettweis et al., 1998). Allen (2000) also indicates that seasonal changes in water viscosity, due to changes in water temperature, can partly explain seasonal variations in SSC in British estuaries. The observed seasonal pattern can also be attributed to sediment transport processes acting within the marsh. Seasonal variations in the growing density and in hydraulic resistance of tidal marsh plants, for example, can play an additional role in reducing suspended sediment input to the centre of the tidal marsh.

Fig. 6. Schematic core logs, presenting the plant debris found in sediment cores taken at the Notelaar marsh: Sa = remains of *Salix* sp. (oblong leaves and wooden debris); Pa = pasture (remains of grasses); Ph = *Phragmites australis* (hollow stems); Sc = *Scirpus* sp. (three-cornered stems and tubers); no = no plant remains (unvegetated tidal flat deposits). The contact elevations between sediment layers containing different plant debris are presented here as the arithmetic mean ± the standard deviation (stddev.) of two series of five cores, one series taken at the old marsh and one at the young marsh. The scale bar on the photographs is subdivided into cm.

### 4.3. Model implementation using empirical input data

The numerical model was applied to the young and old marsh of the Notelaar, using empirical field data as input values for the model parameters (Table 1: model runs 1–4). For both the young and old marsh, the simulation started from the earliest time–elevation point that was reconstructed from the aerial photos and sediment cores: an initial marsh surface elevation $E(0)$ of 4.35 m T.A.W. in 1947 was taken for the young marsh, and 5.20 m T.A.W. in 1958 for the old marsh. In order to solve the model equations, we further needed input values for the rate of organic sediment deposition $dS_{org}/dt$, the compaction rate $dP/dt$ and the sediment parameters $w_s$, $C(0)$ and $\rho$.

$dS_{org}/dt$ incorporates the deposition of organic matter from below-ground roots as well as from above-ground litter. $dS_{org}/dt$ varies in response to the succession of tidal marsh plant communities and to complex variations in their biomass productivity and decay processes, so that at present $dS_{org}/dt$ cannot be modelled in a simple way (Allen, 2000). Following the model applications of Allen (1990) and French (1993) we assume as a first approximation that $dS_{org}/dt$ is constant, which is acceptable for mineral-dominated marshes like the Notelaar marsh. Based on a mean organic matter content of nearly 6%, measured in the sediment cores, and based on the estimated actual growth rate of 0.015 m/yr (averaged for the old and young marsh), $dS_{org}/dt$ is set to $9.10^{-4}$ m/yr. Because the value of $dS_{org}/dt$ is very low, compared to values of $dS_{min}/dt$, $dS_{org}/dt$ will not have an important influence on the vertical growth rate $dE/dt$.

The compaction $dP/dt$ is simulated on a yearly basis, so that compaction of recently deposited sediment, primarily due to sediment dewatering over spring–neap and seasonal cycles, is not included. This effect is in fact already included in the value for the dry bulk density $\rho$ in Eq. 2, which is estimated at 350 kg/m$^3$, based on field measurements at the boring locations. The compaction term $dP/dt$ only includes the compaction of the deposited sediment, after dewatering, under younger sediment load. Both Allen (1990) and French (1993) assume in their model applications that the compaction rate $dP/dt$ after dewatering can be set to zero. For the Notelaar marsh, no significant increase in dry bulk density was observed with increasing depth beneath the marsh surface, indicating that compaction is not an important process. Therefore $dP/dt$ is here set to zero. Cahoon et al. (2000) also showed a close correspondence between sediment accretion and actual elevation change for UK marshes, confirming that compaction in such minerogenic marsh types is not significant. However, on longer time-scales and in more organogenic marsh types compaction can play an important role (Pizzuto and Schwendt, 1997; Allen, 1999, 2000).

To determine the settling velocity $w_s$ of the suspended sediment, we did not carry out direct measurements on the collected suspended sediment samples, partly because of the low sediment concentrations, which would lead to unreliable measurements of $w_s$. Furthermore, such measurements are very difficult for fine-grained estuarine sediments as a consequence of aggregation and formation of flocs, which easily break up when sampled (e.g. Eisma et al., 1997). However, from our measurements, we made an estimation of the in situ settling velocity by inverse modelling. For 44 inundation events, the temporal evolution of the inundation height ($[h(t)-E]$ in Eq. 3) and of the suspended sediment concentration ($C(0)$ and $C(t)$ in Eq. 3) were measured, so that the equivalent $w_s$ can be calculated from Eq. 3 as:

$$w_s = \left[\frac{C(0)}{C(t)} - 1\right] \cdot \frac{dh}{dt} - \frac{[h(t)-E]}{C(t)} \cdot \frac{dC}{dt} \qquad (7)$$

For all these inundation events $w_s$ was computed in time-steps of 300 s and averaged over the whole inundation period. The settling velocity of suspended sediment in estuaries is generally found to increase exponentially with suspended sediment concentration, as a consequence of increased interparticle collisions and flocculation processes (e.g. Krone, 1962; Van Leussen, 1988; Eisma et al., 1997). Krone (1987) also uses this exponential relationship between $w_s$ and $C(t)$ in his salt marsh growth model. However, Fig. 9

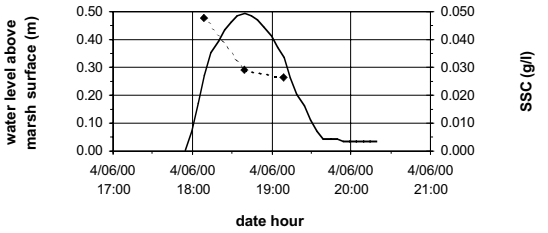


Fig. 7. Example of the temporal variation of the water level above the marsh surface (solid line) and suspended sediment concentration (SSC; broken line) during one tidal inundation of the Notelaar marsh.

shows that there is no clear relationship between the calculated $w_s$ and the initial SSC at the Notelaar marsh. Teeter (2001) also indicates that this relationship disappears for sediment concentrations smaller than 0.100 g/l. Allen (1990) and French (1993) indicate that complex variations in $w_s$ exist in the field, but since the knowledge is at present rather limited, they do not model these variations and instead use a constant median settling velocity $w_s$. Because no detailed data for the Notelaar marsh are available and this study focusses only on long-term suspended sediment modelling, $w_s$ is treated here also as a constant, and is estimated from Fig. 9 to be $10^{-4}$ m/s.

In Eqs. 3 and 4, the suspended sediment concentration $C(0)$ in the flooding water is set to equal $C(t)$ during the ebb tide. During the flood tide, Krone (1987) and French (1993) assume that $C(0)$ has a constant value for all inundation cycles. They both derive a value for $C(0)$ by calibrating their model against an observed record of long-term salt marsh growth. The obtained $C(0)$ value is then used as a constant in all subsequent simulations. Allen (1990) does not model the temporal variation of $C(t)$ during a tidal cycle, like in Eqs. 3 and 4, but only uses Eq. 2 with a sediment concentration $C$, which is assumed to be constant during a tidal cycle. Our field data, however, clearly indicate that $C(t)$, as well as $C(0)$, are not time-independent. $C(t)$ decreases with time during a tidal inundation (Fig. 7) and the initial SSC, at the beginning of marsh inundation, varies linearly with maximum inundation height (Fig. 8). Therefore, $C(0)$ cannot be considered as a constant, but has to be specified as:

$$C(0) = k[h(t_{HW}) - E] \quad (8)$$

where $k$ is a constant, $E$ is the marsh surface elevation and $h(t_{HW})$ is the water level at high tide (both relative to a fixed datum). In order to evaluate the influence of a linear increase of $C(0)$ with inundation height on the modelling results, the model simulations were carried out twice.

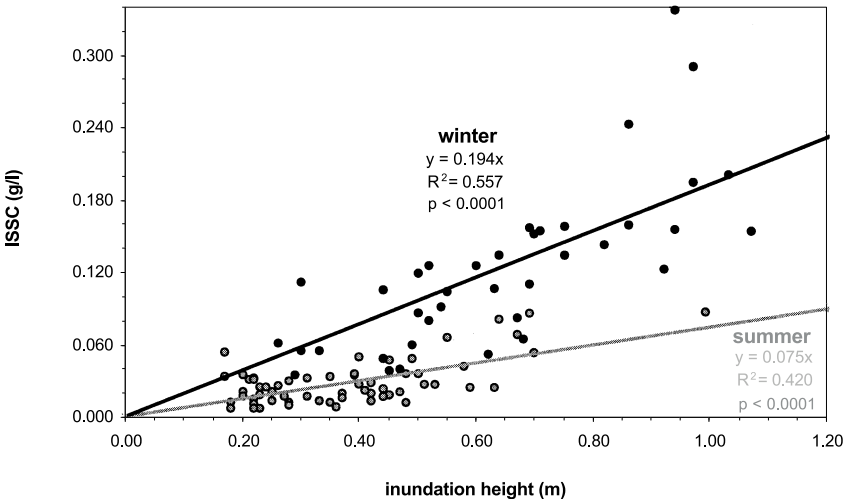


Fig. 8. Linear relationship between initial suspended sediment concentration (ISSC) and inundation height observed for 102 tidal inundations at the Notelaar marsh during a 1-year period (Apr. 2000 to Apr. 2001). Note the difference between summer (Apr.–Sept.) and winter (Oct.–Mar.) observations.

First a constant value for $C(0)$ was used, following Krone (1987) and French (1993). Based on the field measurements, a constant time-averaged $C(0)$ value of 0.040 g/l was chosen, which corresponds with an observed median inundation height of 0.30 m above the surface of the Notelaar marsh (Fig. 8). Secondly, Eq. 8 was incorporated in the model by substitution in Eqs. 3 and 4. Since the deposition rate $dS_{min}/dt$ is calculated by the model on a yearly basis, the observed seasonal variation of $k$ is not modelled but a constant value, averaged over the year, of 0.1345 was derived from the field data (Fig. 8).

### 4.4. Model results and evaluation

For individual inundation events, a continuous decrease of SSC is predicted, which is in good agreement with the field observations (compare Fig. 10a with Fig. 7). Furthermore, the simulated sedimentation rate $dS_{min}/dt$, summed over the whole period of an inundation cycle, increases linearly with maximum inundation height when $C(0)$ is treated as a constant, while an exponential increase is observed when $C(0)$ is defined as a function of inundation height (Fig. 10b). In the latter case, much greater sedimentation rates are predicted, especially for tidal cycles that result in high inundations.

The final modelling results for the young and old marsh of the Notelaar are shown in Fig. 11. The implementation of Krone's model, using a constant $C(0)$ value, results in an important underestimation of the observed growth at the

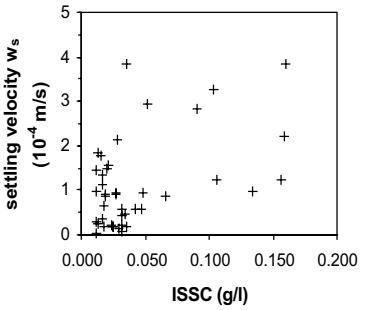


Fig. 9. Variation of settling velocity $w_s$ at the Notelaar marsh as a function of initial suspended sediment concentration (ISSC).

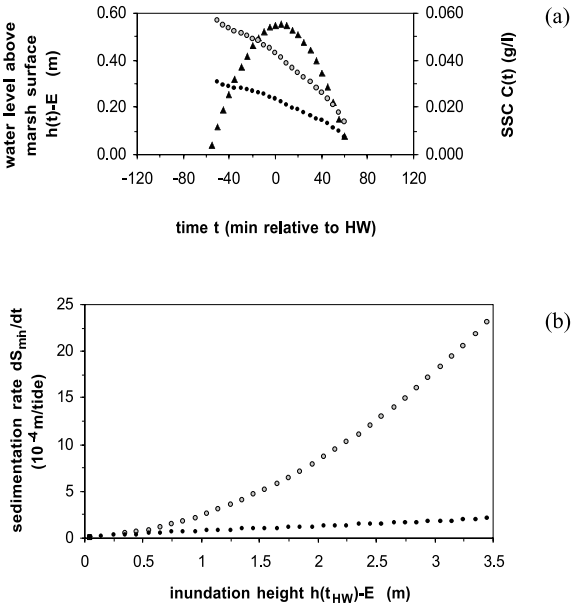


Fig. 10. Comparison of modelling results using a constant $C(0)$ (of 0.040 g/l) (black dots) or $C(0)=k[h(t_{HW})-E)$ ($k=0.1345$) (grey dots): (a) example of predicted tidal curve (triangles) and temporal evolution of suspended sediment concentration SSC (dots) during one tidal inundation with maximum inundation height = 0.55 m; (b) predicted sedimentation rate as a function of inundation height for individual tidal inundations of the marsh surface.

Notelaar marsh, both for the young and for the old marsh. However, when the relationship between $C(0)$ and inundation height is incorporated in the model, the observed vertical growth is very well predicted. The original model of Krone (1987) strongly underestimates the sedimentation rate $dS_{min}/dt$, especially for young marsh surfaces, which have a lower elevation and which are consequently flooded by more and higher tidal inundations (Figs. 10b and 11). His model produces somewhat better results with a constant $C(0)$ value which is about twice the measured mean value of 0.040 g/l, but in this case also his model does not simulate well the strongly asymptotic decrease of the vertical growth rate of the young marsh. This leads to the conclusion that the use of a constant $C(0)$ value results in biased predictions and that the relationship between $C(0)$ and inundation height has to be incorporated in the exist-

Table 1
Summary of model runs and input parameter values

| | Model run | $E(0)$ (m T.A.W.) | Period | MHWL change |
|---|---|---|---|---|
| *Model evaluation* | | | | |
| Old marsh | | | | observed time series (see Fig. 11) |
| (1) | $C(0)$ = constant = 0.040 g/l | 5.20 | 1958–2000 | |
| (2) | $C(0) = k[h(t_{HW}) - E)$ $(k = 0.1345)$ | 5.20 | 1958–2000 | |
| Young marsh | | | | |
| (3) | $C(0)$ = constant = 0.040 g/l | 4.35 | 1947–2000 | |
| (4) | $C(0) = k[h(t_{HW}) - E)$ $(k = 0.1345)$ | 4.35 | 1947–2000 | |
| *Simulations under future sea-level rise* | | | | |
| Young marsh | | | | exponential increase (see Fig. 12) |
| (5) | $C(0)$ = constant = 0.040 g/l | 5.60 | 2000–2100 | |
| (6) | $C(0) = k[h(t_{HW}) - E)$ $(k = 0.1345)$ | 5.60 | 2000–2100 | |

For every model run: $w_s = 10^{-4}$ m/s; $C_s = 350$ kg/m$^3$; $dS_{org}/dt = 6 \times 10^{-4}$ m/yr; $dP/dt = 0$ m/yr.

ing simulation models to predict successfully the vertical growth rate of tidal marshes.

## 5. Discussion

The observed vertical growth of the Notelaar freshwater tidal marsh corresponds very well with the widely expressed idea that low, young salt marshes are characterised by a higher growth rate than high, old marshes. As the marsh surface rises, the growth rate will progressively decrease as a consequence of decreasing frequency and period of tidal inundation (e.g. Steers, 1977; Letzsch and Frey, 1980; Pethick, 1981; Allen and Rae, 1988). The old marsh of the Notelaar has reached an equilibrium level relative to the tidal frame, at an average elevation of 0.1–0.2 m above MHWL, and accumulates as fast as MHWL rises. The young marsh started to grow at a lower elevation. Since then it accumulated very quickly and asymptotically almost up to the equilibrium level of the old marsh (Fig. 11). This is in accordance with the findings of Pethick (1981), who showed that a strongly asymptotic relationship exists between age and elevation of salt marshes in north

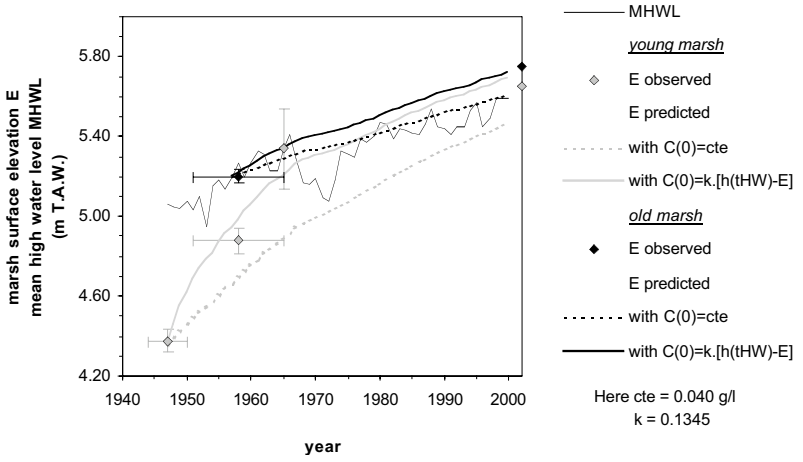


Fig. 11. Observed (symbols) and predicted (lines) vertical growth of the young marsh (in grey) and old marsh (in black) of the Notelaar. Model predictions, with $C(0)$ = constant (= 0.040 g/l) are indicated with broken lines, while predictions with $C(0) = k[h(t_{HW}) - E)$ $(k = 0.1345)$ are indicated with solid lines.

Norfolk (UK). Also, a negative correlation between marsh elevation and sedimentation rate was found in other salt marshes, both from long-term observations (e.g. Allen, 1990; French, 1996) and from short-term measurements (e.g. French, 1993; Allen and Duffy, 1998).

The very fast growth of young freshwater tidal marshes in the Scheldt estuary implies that the inundation frequency and height quickly decrease, and that the initial phase in the vegetation succession with *Scirpus* sp. is consequently rapidly followed by the next phase with *Phragmites australis*. The *Scirpus* phase at the young marsh of the Notelaar had already come to an end at most 15 years after the marsh was formed (Fig. 3). The fast growth of young marshes is one possible explanation why the area of freshwater *Scirpus* marshes is at present so small along the Sea Scheldt, while the older phases with *Phragmites australis* and *Salix* are very common.

The implementation of the model, using Krone's (1987) original mass balance equation with a constant $C(0)$ value, resulted in a clear underestimation of the observed growth of both the young and old marsh of the Notelaar (Fig. 11). We found that the use of a constant value for $C(0)$ is responsible for the failure of the model. Reed (1995), for example, noticed that not only long-term changes in marsh inundation but also changes in suspended sediment concentrations will have an important influence on the long-term response of tidal marsh surfaces. Until now, however, it was found to be very difficult to predict the long-term response of over-marsh suspended sediment concentrations to any changes in marsh inundation height and frequency (Reed, 1995). However, we observed an increase of ISSC with inundation height from short-term field measurements and considered this increase to be the main mechanism controlling long-term changes in ISSC when tidal marsh inundation is changing.

A similar positive linear relationship between ISSC and inundation height was observed by Christiansen et al. (2000) on a coastal salt marsh in Virginia (USA), indicating that this modelling approach is possibly also applicable to other tidal marshes in the world. Furthermore, as discussed above, the long-term asymptotic growth of the Notelaar marsh corresponds very well with long-term accretionary mechanisms reported from other, more marine salt marshes (e.g. Pethick, 1981; Allen, 1990; French, 1996), which further supports the applicability of the model. However, further research is needed to test the possibilities of the presented model structure, to predict observed tidal marsh growth rates at other marsh locations, and to come to a more thorough validation of the model.

For the Notelaar marsh, the main processes that caused changes in tidal marsh inundation, and consequently in suspended sediment supply and deposition, are the vertical rise of the marsh surface and the rising mean high-water level. Other processes, like subsidence or tectonic uplift, were not incorporated in the model, since they are negligible compared with the above-mentioned processes, at least for the Notelaar marsh. However, in other marsh areas in the world, subsidence or tectonic uplift may impact tidal marsh growth (e.g. Sherrod, 2001) as a consequence of increased or decreased marsh inundation, sediment supply, and deposition.

The incorporation of the positive relationship between ISSC and inundation height has important consequences for the existing simulation models and the conclusions resulting from their implementation. The existing models of Krone (1987), Allen (1990, 1995, 1997) and French

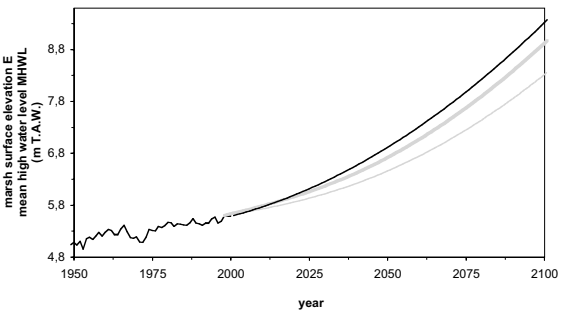


Fig. 12. Simulation of vertical marsh growth for the next century, starting from the observed 2000 elevation of the young marsh of the Notelaar, under a scenario of exponential rise of mean high-water level (thin black line), and using a constant $C(0)$ ($=0.040$ g/l) (thin grey line) or $C(0)=k[h(t_{HW})-E)$ ($k=0.1345$) (solid grey line).

(1993) were specifically used to study the long-term vertical rise of tidal marshes when sea level is rising. Fig. 12 illustrates how the long-term simulation of tidal marsh growth under a future scenario of accelerated sea-level rise is influenced by the use of a constant $C(0)$ or a $C(0)$ as a function of inundation height (see also Table 1, model runs 5 and 6). Several studies, like the modelling study of French (1993) for the salt marshes along the coast of north Norfolk (UK), indicate that marsh vertical growth rates may not be enough to keep pace with future accelerated sea-level rise. The simulations of French (1993) showed that, under the most extreme sea-level rise scenarios, this will result in 'drowning' of tidal marsh vegetation and degradation to bare tidal mud flats. Our simulation model, however, illustrates that, even under an extremely accelerated exponential MHWL rise, degradation of tidal marsh vegetation at the Notelaar marsh will be much longer delayed when the positive correlation between $C(0)$ and inundation height is taken into account (Fig. 12). This correlation is responsible for a strong feedback mechanism through which higher and more frequent marsh inundation results in much higher sedimentation rates. Model simulations, which are based on a constant $C(0)$, result in underestimated sedimentation rates and predictions of exaggeratedly fast tidal marsh degradation. It can therefore be concluded that the long-term over-marsh suspended sediment regime has an important influence on long-term vertical marsh growth and that it is extremely important to incorporate the positive correlation between SSC and marsh inundation to model successfully the long-term behaviour of tidal marsh platforms.

## 6. Conclusions

(1) The long-term vertical growth of fresh-water tidal marshes in the Scheldt estuary is characterised by an asymptotic growth curve. Once a bare tidal mud flat is colonised by plants, the sediment surface rises rapidly due to sedimentation, until a certain level is attained, which is nearly equal to mean high-water level. After that, the growth rate quickly decreases and the marsh surface is slowly built up to an equilibrium level, which is only 10–20 cm higher than mean high-water level. This growth pattern is in accordance with long-term accretionary mechanisms, reported from more marine salt marsh environments.

(2) Intensive short-term field measurements showed that the initial suspended sediment concentration, in the water that floods the marsh surface at the beginning of an inundation, increases linearly with maximum inundation height, at high tide. In addition, this increase is much greater during the winter than during the summer period.

(3) A zero-dimensional time-stepping model successfully simulates the observed long-term historical growth of the Notelaar marsh, using short-term empirical values for the input parameters and incorporating the above-mentioned relationship between sediment concentration and inundation height. Application of the existing models of Krone (1987) and French (1993), without considering this relationship, leads to a strong underestimation of the observed historical growth and leads to biased predictions of vertical marsh growth under future scenarios of sea-level rise. Therefore the observed relationship between sediment concentration and inundation height has to be incorporated to fully explain and successfully simulate the long-term vertical growth of tidal marshes.

## Acknowledgements

This research is funded by the Institute for the Promotion of Innovation by Science and Technology in Flanders (IWT), whose support is gratefully acknowledged. We also thank all the people, and especially Jos Meersmans, who helped with the installation of the automatic measuring station. Erika Van den Bergh gave us permission to use the aerial photograph series, collected at the Institute for Nature Conservation, and Erik Taverniers, of the Waterways and Maritime Affairs Administration, made it possible to use the tidal data. Finally we want to thank the referees, Dr. J.R. French, Dr. R. Gehrels, and an anonymous reviewer, for their constructive comments on the manuscript.

## References


Allen, J.R.L., 1990. Salt-marsh growth and stratification: a numerical model with special reference to the Severn Estuary, southwest Britain. Mar. Geol. 95, 77–96.

Allen, J.R.L., 1994. A continuity-based sedimentological model for temperate-zone tidal salt marshes. J. Geol. Soc. 151, 41–49.

Allen, J.R.L., 1995. Salt-marsh growth and fluctuating sea-level: implications of a simulation model for Flandrian coastal stratigraphy and peat-based sea-level curves. Sediment. Geol. 100, 21–45.

Allen, J.R.L., 1997. Simulation models of salt-marsh morphodynamics: some implications for high-intertidal sediment couplets related to sea-level change. Sediment. Geol. 113, 211–223.

Allen, J.R.L., 1999. Geological impacts on coastal wetland landscapes: some general effects of sediment autocompaction in the Holocene of northwest Europe. Holocene 9, 1–12.

Allen, J.R.L., 2000. Morphodynamics of Holocene salt marshes: a review sketch from the Atlantic and Southern North Sea coasts of Europe. Quat. Sci. Rev. 19, 1155–1231.

Allen, J.R.L., Duffy, M.J., 1998. Medium-term sedimentation on high intertidal mudflats and salt marshes in the Severn Estuary, SW Britain: the role of wind and tide. Mar. Geol. 150, 1–27.

Allen, J.R.L., Pye, K., 1992. Coastal saltmarshes: their nature and importance. In: Allen, J.R.L., Pye, K. (Eds.), Saltmarshes: Morphodynamics, Conservation and Engineering Significance. Cambridge University Press, Cambridge, pp. 1–18.

Allen, J.R.L., Rae, J.E., 1988. Vertical salt-marsh accretion since the Roman Period in the Severn Estuary, southwest Britain. Mar. Geol. 83, 225–235.

Baeyens, W., Van Eck, B., Lambert, C., Wollast, R., Goeyens, L., 1998. General description of the Scheldt estuary. Hydrobiologia 366, 1–14.

Baumann, R.H., Day, J.W., Miller, C.A., 1984. Mississippi deltaic wetland survival: sedimentation versus coastal submergence. Science 224, 1093–1095.

Cahoon, D.R., French, J.R., Spencer, T., Reed, D., Möller, I., 2000. Vertical accretion versus elevational adjustment in UK saltmarshes: an evaluation of alternative methodologies. In: Pye K., Allen, J.R.L. (Eds.), Coastal and Estuarine Environments: Sedimentology, Geomorphology and Geoarchaeology. The Geological Society, London, pp. 223–238.

Christiansen, T., Wiberg, P.L., Milligan, T.G., 2000. Flow and sediment transport on a tidal salt marsh surface. Estuar. Coast. Shelf Sci. 50, 315–331.

Claessens, J., Meyvis, L., 1994. Overzicht van de tijwaarnemingen in het Zeescheldbekken gedurende het decennium 1981–1990. Ministerie van de Vlaamse Gemeenschap AWZ Afdeling Maritieme Schelde, Antwerpen.

Criel, B., Muylaert, W., Hoffmann, M., De Loose, L., Meire, P., 1999. Vegetatiemodellering van de buitendijkse gebieden langs de Zeeschelde. Raport OMES DS7.2, Instituut voor Natuurbehoud, Brussels.

De Ferraris, J., 1774–1777. Kabinetskaart van de Oostenrijkse Nederlanden. Reprint on scale 1:25.000. Gemeentekrediet, Brussels.

Durinck, P., 1981. Het getijderivierengebied in ons land. Natuurreservaten 4bis, 60–68.

Eisma, D., Dyer, K.R., Van Leussen, W., 1997. The in-situ determination of the settling velocities of suspended fine-grained sediment - a review. In: Burt, N., Parker, R. Watts, J. (Eds.), Cohesive Sediments. Wiley, Chichester, pp. 17–44.

Fettweis, M., Sas, M., Monbaliu, J., 1998. Seasonal, neap-spring and tidal variation of cohesive sediment concentration in the Scheldt Estuary, Belgium. Estuar. Coast. Shelf Sci. 47, 21–36.

French, J.R., 1993. Numerical simulation of vertical marsh growth and adjustment to accelerated sea-level rise, north Norfolk, U.K. Earth Surf. Process. Landforms 18 (1), 63–81.

French, J.R., Spencer, T., 1993. Dynamics of sedimentation in a tide-dominated backbarrier salt marsh, Norfolk, U.K. Mar. Geol. 110, 315–331.

French, J.R., Spencer, T., Murray, A.L., Arnold, N.S., 1995. Geostatistical analysis of sediment deposition in two small tidal wetlands, Norfolk, United Kingdom. J. Coast. Res. 11, 308–321.

French, P.W., 1996. Implications of a saltmarsh chronology for the Severn Estuary based on independent lines of dating evidence. Mar. Geol. 135, 115–125.

Hoffmann, M., 1993. Vegetatiekundig-ecologisch onderzoek van de buitendijkse gebieden langs de Zeeschelde met vegetatiekartering. Universiteit Gent, Gent.

Hoffmann, M., Graré, W., Meire, P., 1997. De oevers langs de Zeeschelde: van uniformiteit naar structuurdiversiteit. Water 95, 131–137.

Kearny, M.S., Stevenson, J.C., 1991. Island land loss and marsh vertical accretion rate: evidence for historical sea-level changes in Chesapeake Bay. J. Coast. Res. 7, 403–415.

Krone, R.B., 1962. Flume studies of the transport of sediment in estuarial shoaling processes. University of California, Hydraulic Engineering Laboratory and Sanitary Engineering Research Laboratory, Berkeley.

Krone, R.B., 1987. A method for simulating historic marsh elevations. In: Kraus, N.C. (Ed.), Coastal Sediments '87. American Society of Civil Engineers, New York, pp. 316–323.

Leonard, L.A., 1997. Controls of sediment transport and deposition in an incised mainland marsh basin, southeastern North Carolina. Wetlands 17, 263–274.

Leonard, L.A., Luther, M.E., 1995. Flow hydrodynamics in tidal marsh canopies. Limnol. Oceanogr. 40, 1474–1484.

Letzsch, W.S., Frey, R.W., 1980. Deposition and erosion in a Holocene salt marsh, Sapelo Island, Georgia. J. Sediment. Petrol. 50, 529–542.

Meire, P., Rossaert, G., De Regge, N., Ysebaert, T., Kuijken, E., 1992. Het Schelde-estuarium: ecologische beschrijving en

een visie op de toekomst. Instituut voor Natuurbehoud, Hasselt.

Orson, R.A., Warren, R.S., Niering, W.A., 1998. Interpreting sea-level rise and rates of vertical marsh accretion in a southern New England tidal salt marsh. Estuar. Coast. Shelf Sci. 47, 419–429.

Pethick, J.S., 1981. Long-term accretion rates on tidal salt marshes. J. Sediment. Petrol. 51, 571–577.

Pethick, J.S., Leggett, D., Husain, L., 1990. Boundary layers under salt marsh vegetation developed in tidal currents. In: Thornes J.B. (Ed.), Vegetation and Erosion. Wiley, Chichester, pp. 113–124.

Pizzuto, J.E., Schwendt, A.E., 1997. Mathematical modeling of autocompaction of a Holocene transgressive valley-fill deposit, Wolfe Glade, Delaware. Geology 25, 57–60.

Reed, D.J., 1993. Hydrology of temperate wetlands. Prog. Phys. Geogr. 17, 20–31.

Reed, D.J., 1995. The response of coastal marshes to sea-level rise: survival or submergence? Earth Surf. Process. Landforms 20, 39–48.

Sherrod, B.L., 2001. Evidence for earthquake-induced subsidence about 1100 yr ago in coastal marshes of southern Puget Sound, Washington. Geol. Soc. Am. Bull. 113, 1299–1311.

Shi, Z., 1993. Recent saltmarsh accretion and sea-level fluctuations in the Dyfi Estuary, central Cardigan Bay, Wales, UK. Geo-Mar. Lett. 13, 182–188.

Shi, Z., Hamilton, L.J., Wolanski, E., 2000. Near-bed currents and suspended sediment transport in saltmarsh canopies. J. Coast. Res. 16, 909–914.

Steers, J.A., 1977. Physiography. In: Chapman, V.J. (Ed.), Wet Coastal Ecosystems. Elsevier Science, Amsterdam, pp. 31–60.

Teeter, A.M., 2001. Clay-silt sediment modeling using multiple grain classes. Part I: Settling and deposition. In: McAnally, W.H., Mehta, A.J. (Eds.), Coastal and Estuarine Fine Sediment Processes. Elsevier Science, Amsterdam, pp. 157–171.

Van Damme, S., De Winder, B., Ysebaert, T., Meire, P., 2001. Het 'bijzondere' van de Schelde: de abiotiek van het Schelde-estuarium. Levende Natuur 102, 37–39.

Van Eck, G.T., De Pauw, N., Van Langenbergh, M., Verreet, G., 1991. Emissies, gehalten, gedrag en effecten van (micro)-verontreiningingen in het stroomgebied van de Schelde en het Schelde-estuarium. Water 60, 84–99.

Van Leussen, W., 1988. Aggregation of particles, settling velocity of mud flocs - a review. In: Dronkers, J., Van Leussen, W. (Eds.), Physical Processes in Estuaries. Springer, Berlin, pp. 347–403.

Vandermaelen, P., 1846–1854. Carte topographique de la Belgique. Scale 1:20.000. l'Etablissement Géographique de Bruxelles, Brussels.

Walker, H.J., Coleman, J.M., Roberts, H.H., Tye, R.S., 1987. Wetland loss in Louisiana. Geogr. Ann. 69A, 189–200.

Ward, L.G., Kearney, M.S., Stevenson, J.C., 1998. Variations in sedimentary environments and accretionary patterns in estuarine marshes undergoing rapid submergence, Chesapeake Bay. Mar. Geol. 151, 111–134.

Woolnough, S.J., Allen, J.R.L., Wood, W.L., 1995. An exploratory numerical model of sediment deposition over tidal marshes. Estuar. Coast. Shelf Sci. 41, 515–543.